*Article*

# Observation of ultrashort laser pulse evolution in silicon photonic crystal waveguide

**Xiaochun Wang [1], Jiali Liao [2], Jinghan Pan [1], Heng Yang [3] and Xiujian Li [1,*]**

[1] Department of Physics, College of Liberal Arts and Sciences, National University of Defense Technology, Changsha, 410073, China; xiaochunwang01@163.com (X.W.); panjinghan18@nudt.edu.cn (J.P.);
[2] School of Physics and Optoelectronic Engineering, Xidian University, Xi'an, 710071, China; liaojiali@xidian.edu.cn
[3] College of information and communication, National University of Defense Technology, Changsha, 410073, China; hengy@yeah.net
* Correspondence: xjli@nudt.edu.cn

**Abstract:** Based on the sensitive sum frequency generation cross-correlation frequency-resolved optical gating (SFG-XFROG) measurement setup, besides the pulse broadening, blue shift, red shift and obvious pulse acceleration, we observed the soliton evolution when the low energy soliton pulse with wavelength of 1555nm transmit through the Si photonic crystal waveguide. The measurements were nicely matched with the simulation results, which are achieved with an optimized nonlinear Schrödinger equation (NLSE) modeling. The effects of various parameters of the silicon photonic crystal waveguides and the incident pulses on the pulse transmission were also analyzed, including the nonlinear effects and dispersion such as the self-phase modulation (SPM), self-steepening (SS) and intra-pulse Raman scattering(IRS). The results help us understand further the ultra-fast nonlinear dynamics of soliton in silicon-based waveguides, and even open a novel way for soliton-based functional elements in CMOS-compatible platforms.

**Keywords:** Photonic crystal waveguide; Pulse acceleration; Self-steepening; Self-phase modulation



**Citation:** Wang, X.; Liao J.; Pan J.; Yang H.; Li X. Observation of ultrashort laser pulse evolution in silicon photonic crystal waveguide. *Preprints* **2021**, *1*, 0. https://doi.org/

Received:
Accepted:
Published:



## 1. Introduction

With the capability to tightly confine optical modes [1], the compatibility with mature CMOS technologies [2], and the extremely large nonlinearities enhanced by slow-light effects, the Si photonic crystal waveguides (PhCWs) have been attracting more and more intention. Four-wave-mixing, temporal soliton, optical filter, all-optical modulation, all-optical switching, ultralow-power all-optical signal processing and all-optical wavelength conversion have been demonstrated in Si PhCWs [1,3]. Basically, pulses propagation is affected by the nonlinear properties and the inherent dispersion of the Si PhCWs, and they can make the pulses propagation exhibit optical solitons effects at the anomalous dispersion region [4], which will be important carriers for Numerous applications of optical information processing [5–8]. Recently, the nonlinear effects such as the group velocity dispersion (GVD), the self-phase modulation (SPM), two photon absorption (TPA), cross phase modulation (XPM) and so on have been widely studied [9–13]. As the solitons are the nonlinear waves that exhibit invariant or recurrent behavior as they propagate through some materials [14,15] by precise control of dispersion and nonlinear effects to govern solitons propagation can implement wide applications [16,17].

Actually, the FROG and SFG-XFROG are efficient tools for check ultra-short laser pulses [18–20]. However, up to now, though we had checked the soliton behavior in the Si nanowire and PhCWs [21–26], it's still unclear about all details of the soliton propagation, especially when and how the low energy soliton will be compressed and split in the Si PhCWs which usually are considered to be suitable for managing the solitons than the Si nanowire [27].

Herein, based on a sensitive SFG-XFROG ultra-short laser pulse measurement setup, we observed that the pulses blue shift, red shift and pulse shaping in Si PhCWs with ultralow input pulse energy. Furthermore, the experimental results are nicely agreed with

the optimized nonlinear Schrödinger equation (NLSE) modeling simulation results. We simulate the nonlinear effect and the dispersion effect on the propagation in the Si PhCWs. The research results will provide valuable information for the design of waveguides [28] for various on-chip photonic circuits, which is necessary for the ultra-broadband high-speed optical communications and optical signal processing.

## 2. Measurement setup and observations of pulse transmission

The experimental measurement setup with SFG-XFROG for Si PhCWs chip measurements are shown in Fig. 1.

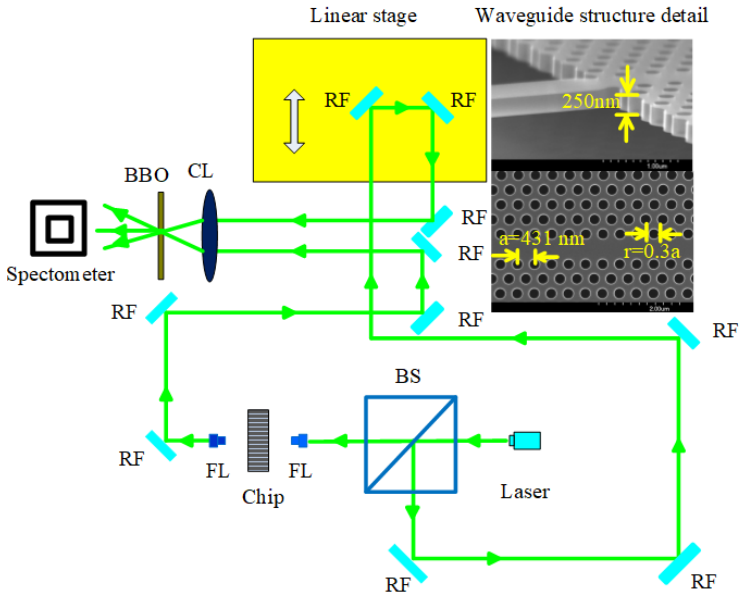


**Figure 1.** Experimental measurement setup with SFG-XFROG and the Si PhCWs detail. RF: Reflector, BS: Beam splitter, FL: Focusing lens, CL: Bi-convex lens, BBO: Barium borate crystal.

The SFG-XFROG measurement setup provides sensitive and accurate measurement of the temporal domains and spectral domains of the optical pulses output from the silicon photonic crystal waveguides. In the setup, a BBO crystal (1mm thickness, provided by CASTECH INC. CHINA) and a Horiba JY FHR1000 spectrometer with a SYMPHONY II UVCCD-1024x256-BIDD detector work well, which enable the minimum detected pulse energy be down to about 500 attojoule (aJ), the spectral resolution be better than 0.1nm, and the time resolution short to less than 1 femtosecond (fs). Anyway, the measurement setup ensures the ultrashort pulse profiles including complex time and frequency properties be measured nicely, which help us to capture the soliton dynamics.

The Si PhCWs are laid out on a SOI chip (structure details are shown in Fig. 1, with 250nm top Si layer, 3 um buried silica and 500 um Si substrate. The ultrashort pulses are input to the Si PhCWs in TE polarization, which is 1.3 mm long, with a=431 nm, and r=129nm. For the Si PhCWs in the experiment, the group velocity dispersion (GVD) $\beta_2$ is -1800 $ps^2/m$ and the third order dispersion (TOD) $\beta_3$ is 0.6 $ps^3/m$ in the wavelength of 1555nm [26].

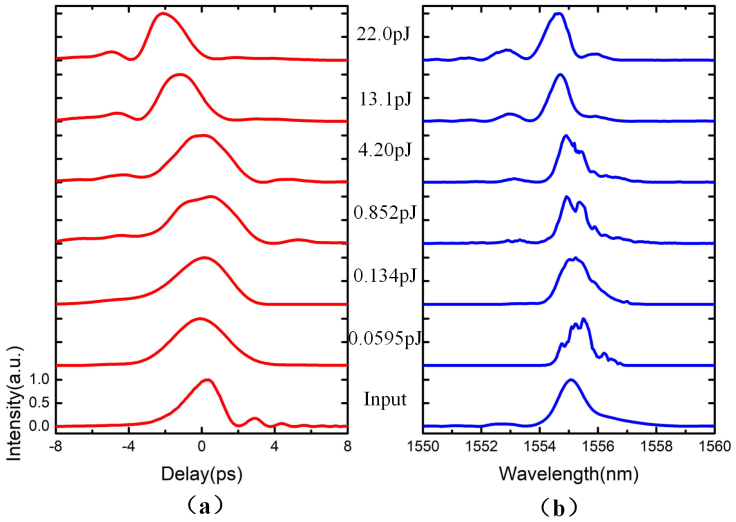


**Figure 2.** The output SFG-XFROG measurements, (a) is the normalized intensity profiles in temporal domain; (b) is the normalized intensity profiles in spectral domain.

The pulse duration of the input laser pulse provided by a fiber laser is FWHM=2.25 ps, which is measured at central wavelength 1555 nm. The pulse energy will be changed for the measurements, and the corresponding output pulse profiles measured by the SFG-XFROG are shown in Fig.2, in which the normalized pulse intensities in temporal domain and spectral domain are laid out.

The experimental results shows that the output pulse has been broadened in Fig.2(a), and the broadening of the output pulse FWHM becomes weaken from 3.91ps to 2.21ps with the increasing of the input energy. And the broadening factor is from 1.74 to 0.98 with the energy increased to 22.0pJ. Then the output pulse have a 1.8 compression factor with the increased of pulse energy from 59.5fJ to 22.0pJ. The FWHM is effected by the energy of the input pulse. The output pulse appeared obvious pulse acceleration. And the largest pulse acceleration was 2.17ps with 22.0pJ input energy. And the out pulse was still smooth and wasn't destroyed in the experiment.

The Fig.2(b) shows the normalized intensity profiles in spectral domain. The frequency domain centroid showed red shift with the low input pulse energy and blue shift with the high input pulse energy in Fig.2(b). The largest red shift was 0.41nm on the output pulse centroid 1555.41nm with 59.5fJ input energy. And the largest blue shift was 0.68nm on the output pulse centroid 1554.32nm with 22.0pJ input energy. The blue shift is caused by the free carriers dispersion (FCD) in Si PhCWs [26]. With the increasing of the input pulse energy the free carries increased, and the FCD increased. Then the blue shift become obviously.

## 3. Optimized NLSE modeling simulations and discussions

In order to try out the major factors for the broadening and shift as shown in Fig.2, we perform the optimized nonlinear Schrödinger equation (NLSE) modeling simulations [26].

$$\frac{\partial A}{\partial z} + i\frac{\beta_2}{2}\frac{\partial^2 A}{\partial^2 t} - \frac{\alpha_{eff}}{2}A = i(\gamma_{eff} - \alpha_{TPA.eff})|A|^2 A + (ik_0 k_{c.eff} - \frac{\sigma_{eff}}{2})N_c A \quad (1)$$

$$\frac{\partial N_c(z,t)}{\partial t} = \frac{\alpha_{TPA.eff}}{2h\nu_0}|A(z,t)|^4 - \frac{N_c(z,t)}{\tau_c} \quad (2)$$

The Kerr coefficient is 1.02 $10^3$ (1/W/m), the effective TPA coefficients is 13.4 $10^{-12}$ m/W for 1555nm, $k_{c.eff} = -13.3\ 10^{27}$ $m^3$ and $\sigma_{eff}$=4.6 $10^{-21}$ $m^2$ are the effective parameter [26].

Fig.3 shows the experimental and the optimized NLSE simulation results for 1555nm with 0.134pJ and 22.0pJ input pulse energy. In the simulations, the input pulse profiles measured by SFG-XFROG are input as the intensity and phase of the initial pulse. Obviously, the experimental results are remarkably matched with the NLSE simulation results nicely, which indicates that the optimized NLSE modeling and the parameters are suitable for the Si PhCWs. Anyway, the matching of the NLSE simulation results and the measurements ensure that, the NLSE modeling simulation can properly predict pulse dynamics in the Si PhCWs, which will be helpful for demonstrating the pulse dynamics beyond experiments here.

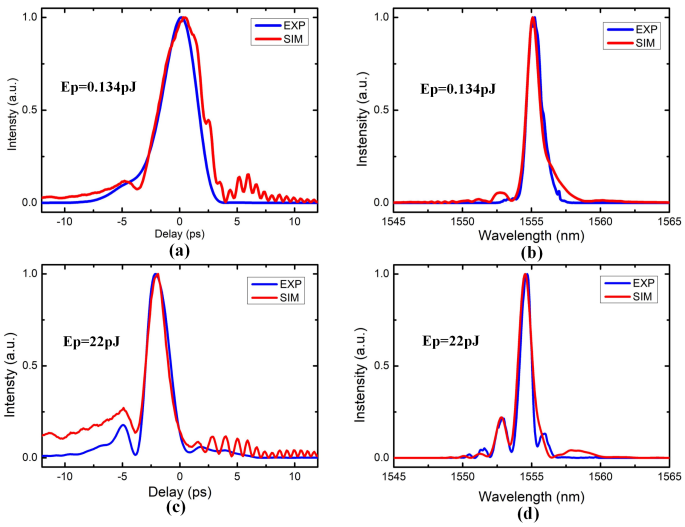


**Figure 3.** The experimental and the optimized NLSE simulation results for various pulse energies, (a) and (c) temporal profiles , (b) and (d) spectral profiles of the pulse, (a) and (b) with 0.134pJ input pulse energy, (c) and (d) with 22.0pJ input pulse energy. The blue solid line are experimental results, and the red solid line are optimized NLSE simulation results.

The propagation of optical pulses can be modeled by NLSE in which the Si PhCWs is functioned far from the band edge of the waveguide. This section may be divided by subheadings. It should provide a concise and precise description of the experimental results, their interpretation as well as the experimental conclusions that can be drawn.

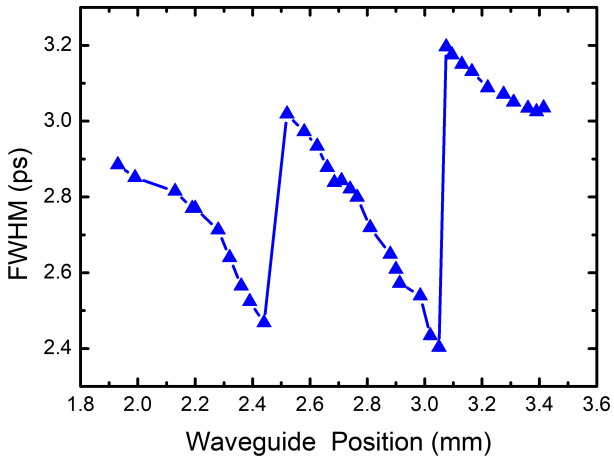


**Figure 4.** The output pulse FWHM simulated by the NLSE simulation with different waveguide position in 1555nm with 22.0pJ input pulse energy.

The simulation input pulse was the experiment input pulse above with 22.0pJ with center wavelength 1555nm in the PhCWs. Set the different gradual change Si PhCW length to simulate the output pulse, the same as the pulse propagation outline in the Si PhCW at different position. Fig.4 shows the FWHM of the pulse propagating through the Si PhCW. Fig.4 shows that the pulse FWHM was transformed periodic in the propagation. When the FWHM is gradually compressed to the narrowest, sudden broadening occurs in the transmission. Because of the large pulse loss in the transmission process, the relative width of the pulse width increases in the longer position of the waveguide. The the pulse transmission emerged the soliton with the balance between the nonlinear effects and the dispersion in the Si PhCW.

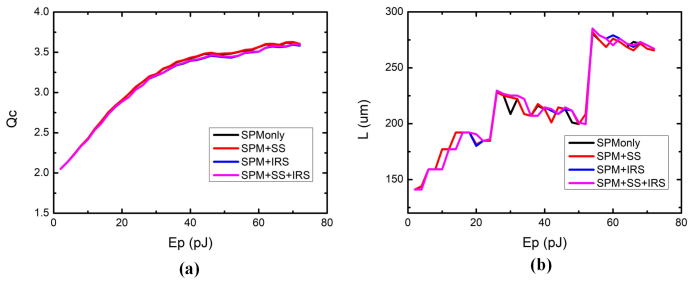


**Figure 5.** The compression factor (Qc) and the narrowest pulse compression position with different input pulse energy (Ep) in 1550nm with 2.4ps in the Si PhCWs simulated by NLSE.

Fig.5 simulated the input pulse with 1550nm transmit in the Si PhCW above. The simulation considered as SPM only, SPM and SS, SPM and IRS, SPM and SS and IRS. Fig.5(a) shows that the input pulse energy effect the pulse compression and the self-steepening have no effect on the pulse compression, and the intrapulse Raman scattering effect the pulse compression obviously by simulation. Fig.5(b) shows that position of the narrowest compression in the Si PhCW at different input pulse energy and different nonlinear condition. The self-steepening and the intrapulse Raman scattering have no effect on the narrowest compress position. It effected by the input energy and the position have a platform. And the narrowest compress position shows as step-form change. The Si PhCW can be designed at the platform for compress a certain range energy of the pulse.

## 4. Conclusions

In summary, according to the sensitive SFG-XFROG measurements, we observed that the ultrashort laser pulse have broadened with broaden factor 1.74, blue shift, red shift and obvious pulse acceleration when the temporal soliton transmit through the Si PhCW at center wavelength of 1555nm. The optimized NLSE simulation results matched the measurements nicely. The results shows that FWHM of pulse present sudden change at the narrowest to the nest period. And the simulation results shows that periodic solitons are produced in the process of pulse transmission at center wavelength of 1555nm. The input pulse energy affects the pulse compression, while the self-steepening has no effect on the pulse compression. According to the simulation, obviously the intra-pulse Raman scattering affects the pulse compression, while the self-steepening and the intra-pulse Raman scattering have no effect on the narrowest compress position. Through the study we can optimize the Si PhCWs for pulse shaping. This analysis results help us understand further how the ultra-fast pulses propagate in silicon-based waveguides, and even open the way for soliton-based functional elements in CMOS-compatible platforms..

**Author Contributions:** "Conceptualization, Li, X. and Wang X.; methodology, Wang X.; software, Liao J.; validation, Wang X.; investigation, Pan J. and Wang X.; data curation, Wang X.; writing, all authors; supervision, Li X. All authors have read and agreed to the published version of the manuscript."

**Funding:** "This research was funded by the National Science Foundation of China (NSFC) (61070040, 61108089, 61205087, 61107005 62005207), Hunan Provincial Natural Science Foundation of China (805297133191), Natural Science Foundation of Shaanxi Province (2019JQ-648).

**Conflicts of Interest:** "The authors declare no conflict of interest."

## References

1. V. R. Almeida, C. A. Barrios, R. R. Panepucci, and M. Lipson, All-optical control of light on a silicon chip, *Nature* **2004**, *431*, 1081-1084.
2. D. Dai, and J. E. Bowers, Novel concept for ultracompact polarization splitter-rotator based on silicon nanowires, *Optics Express* **2011**, *19*, 10940-10949.
3. M. A. Foster, A. C. Turner, J. E. Sharping, B. S. Schmidt, M. Lipson, and A. L. Gaeta, Broad-band optical parametric gain on a silicon photonic chip, *Nature* **2006**, *441*, 960-963.
4. G. P. Agrawal, Chapter 2 - Pulse Propagation in Fibers, in Nonlinear Fiber Optics (Fourth Edition, ), *Academic Press, San Diego* **2006**.
5. J. Koch, S. Li, and S. Pachnicke, Transmission of Higher Order Solitons Created by Optical Multiplexing, *J. LIGHTWAVE TECHNOL.* **2019**, *37* 933-941.
6. E. V. Sedov, A. A. Redyuk, M. P. Fedoruk, A. A. Gelash, L. L. Frumin, and S. K. Turitsyn, Soliton content in the standard optical OFDM signal, *OPT. LETT.* **2018**, *43* 5985-5988.
7. D. Marpaung, M. Pagani, B. Morrison, and B. J Eggleton, Nonlinear Integrated Microwave Photonics, *J. LIGHTWAVE TECHNOL.* **2014**, *32* 3421-3427.
8. X. Zou, B. Lu, W. Pan, L. Yan, A. Stöhr, and J. Yao, Photonics for microwave measurements, *LASER PHOTONICS REV.* **2016**, *10* 711-734.
9. T. Nakahama, N. Ozaki, H. Oda, N. Ikeda, and Y. Sugimoto, Numerical investigation of highly efficient and tunable terahertz-wave generation using a low-group-velocity and low-dispersion two-dimensional GaAs photonic crystal waveguide, *JPN. J. APPL. PHYS.* **2020**, *59* 90903.
10. I. Hsieh, X. Chen, J. I. Dadap, N. C. Panoiu, R. M. Osgood, S. J. McNab, and Y. A. Vlasov, Ultrafast-pulse self-phase modulation and third-order dispersion in Si photonic wire-waveguides, *OPT. EXPRESS* **2006**, *14* 12380-12387.
11. D. Chaturvedi, A. K. Mishra, and A. Kumar, Self-phase modulation-induced modulation instability in silicon-on-insulator nano-waveguides, *Optics & Laser Technology* **2019**, *119* 105578.
12. M. Pu, H. Hu, L. Ottaviano, E. Semenova, D. Vukovic, L. K. Oxenløwe, and K. Yvind, Ultra-Efficient and Broadband Nonlinear AlGaAs-on-Insulator Chip for Low-Power Optical Signal Processing, *LASER PHOTONICS REV.* **2018**, *12* 1800111.
13. K. J. A. Ooi, D. K. T. Ng, T. Wang, A. K. L. Chee, S. K. Ng, Q. Wang, L. K. Ang, A. M. Agarwal, L. C. Kimerling, and D. T. H. Tan, Pushing the limits of CMOS optical parametric amplifiers with USRN:$Si_7N_3$ above the two-photon absorption edge, *NAT. COMMUN.* **2017**, *8* 13878.
14. P. Colman, C. Husko, S. Combrié, I. Sagnes, C. W. Wong, and A. De Rossi, Temporal solitons and pulse compression in photonic crystal waveguides, *NAT. PHOTONICS* **2010**, *4* 862-868.
15. A. Blanco-Redondo, C. Husko, D. Eades, Y. Zhang, J. Li, T. F. Krauss, and B. J. Eggleton, Observation of soliton compression in silicon photonic crystals, *NAT. COMMUN.* **2014**, *5* 3160.
16. J. Liu, A. S. Raja, M. Karpov, B. Ghadiani, M. H. P. Pfeiffer, B. Du, N. J. Engelsen, H. Guo, M. Zervas, and T. J. Kippenberg, Ultralow-power chip-based soliton microcombs for photonic integration, *OPTICA* **2018**, *5* 1347-1353.
17. S. Soysouvanh, M. A. Jalil, I. S. Amiri, J. Ali, G. Singh, S. Mitatha, P. Yupapin, K. T. V. Grattan, and M. Yoshida, Ultra-fast electro-optic switching control using a soliton pulse within a modified add-drop multiplexer, *Microsystem Technologies* **2018**, *24* 3777-3782.
18. A. Efimov, and A. J. Taylor, Cross-correlation frequency-resolved optical gating for studying ultrashort-pulse nonlinear dynamics in arbitrary fibers, *APPL. OPTICS* **2005**, *44* 4408-4411.
19. J. M. Dudley, X. Gu, L. Xu, M. Kimmel, E. Zeek, P. O Shea, R. Trebino, S. Coen, and R. S. Windeler, Cross-correlation frequency resolved optical gating analysis of broadband continuum generation in photonic crystal fiber: simulations and experiments, *OPT. EXPRESS* **2002**, *10* 1215-1221.
20. N. Tsurumachi, K. Hikosaka, X. Wang, M. Ogura, N. Watanabe, and T. Hattori, Observation of ultrashort pulse propagation anisotropy in a semiconductor quantum nanostructure optical waveguide by cross-correlation frequency resolved optical gating spectroscopy, *J. APPL. PHYS.* **2003**, *94* 2616-2621.
21. M. Marko, A. Veitia, X. Li, and J. Zheng, Disturbance of soliton pulse propagation from higher-order dispersive waveguides, *APPL. OPTICS* **2013**, *52* 4813-4819.
22. J. Liao, M. Marko, X. Li, H. Jia, J. Liu, Y. Tan, J. Yang, Y. Zhang, W. Tang, M. Yu, G. Lo, D. Kwong, and C. W. Wong, Cross-correlation frequency-resolved optical gating and dynamics of temporal solitons in silicon nanowire waveguides, *OPT. LETT.* **2013**, *38* 4401-4404.
23. M. D. Marko, X. Li, J. Zheng, J. Liao, M. Yu, G. Lo, D. Kwong, C. A. Husko, and C. Wei Wong, Phase-resolved observations of optical pulse propagation in chip-scale silicon nanowires, *APPL. PHYS. LETT.* **2013**, *103* 21103.

24. M. Marko, X. Li, and J. Zheng, Soliton propagation with cross-phase modulation in silicon photonic crystal waveguides, *Journal of the Optical Society of America B* **2013**, *30* 2100-2106.
25. K. Liu, J. F. Zhang, W. Xu, Z. H. Zhu, C. C. Guo, X. J. Li, and S. Q. Qin, Ultra-fast pulse propagation in nonlinear graphene/silicon ridge waveguide, *SCI. REP-UK* **2015**, *5* 16734.
26. X. Li, J. Liao, Y. Nie, M. Marko, H. Jia, J. Liu, X. Wang, and C. W. Wong, Unambiguous demonstration of soliton evolution in slow-light silicon photonic crystal waveguides with SFG-XFROG, *OPT. EXPRESS* **2015**, *23* 10282-10292.
27. J. Zhang, Q. Lin, G. Piredda, R. W. Boyd, G. P. Agrawal, and P. M. Fauchet, Optical solitons in a silicon waveguide, *OPT. EXPRESS* **2007**, *15* 7682-7688.
28. M. Fu, J. Liao, Z. Shao, M. Marko, Y. Zhang, X. Wang, and X. Li, Finely engineered slow light photonic crystal waveguides for efficient wideband wavelength-independent higher-order temporal solitons, *APPL. OPTICS* **2016**, *55* 3740-3745.